METALLURGICAL ASPECTS OF FORGE MODELLING IN ALLOY 718

P.E. MOSSER*, G. LECONTE*, J. LERAY**, A. LASALMONIE*, Y. HONNORAT**

Material and Process Laboratory
SNECMA - Direction Technique
* B.P. 48 - 92234 GENNEVILLIERS CEDEX FRANCE
** B.P. 81 - 91003 EVRY CEDEX FRANCE

Abstract

Alloy 718 is a widely used alloy in SNECMA's engines for applications in forged rotating parts. The most important mechanical property, low cycle fatigue, depends strongly on grain size, which results directly from the forging process. Metallurgical data have been coupled with FORGE2^R metal flow numerical results to give a prediction of grain size in recrystallized and dead zones. After calibration, using measurements on forged parts, this approach proved to be an efficient metallurgical forge modelling.

Introduction

Alloy 718 is a widely used alloy in SNECMA's engines for applications in forged disks and rotating parts. The major concern with the mechanical properties of these parts is high temperature low cycle fatigue (LCF) resistance, which depends strongly on the grain size (fig. 1). The required fine grained microstructure is obtained during the forging operations. Through the years, parts were submitted to higher stresses and temperatures. This lead to improve material ability through changes of the forging practices. Altogether there was an increasing need at SNECMA forge shop for a forge process modelling which would give, not only a description of metal flow, but also a prediction of the microstructure, and hence of the mechanical properties, in every location of the forged part.

This paper is a presentation of such a model, developped mainly in SNECMA's laboratory. From the metallurgical evolution obtained through thermomechanical testings, microstructure prediction rules are deduced which can be applied to finite element flow modelling results. A real disk forging is confronted with the microstructural prediction.

Metallurgical data

The microstructure of Alloy 718 may be described by grain size distribution, residual cold work, δ phase amount and morphology, γ'' amount and size, carbides, and dendritic segregation. A detailed microstructure description is very difficult and useless for the forge metallurgist.As LCF

Superalloy 718—Metallurgy and Applications
Edited by E.A. Loria
The Minerals, Metals & Materials Society, 1989

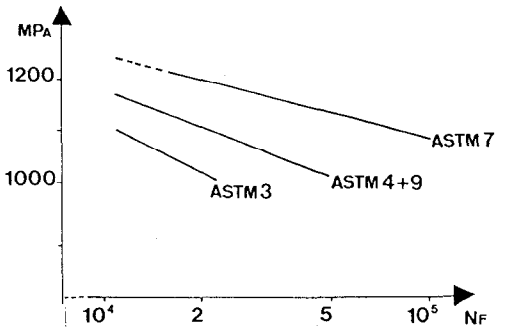

Fig.1: LCF properties vs grainsize
Nf number of cycles to failure at 550°C–R =0

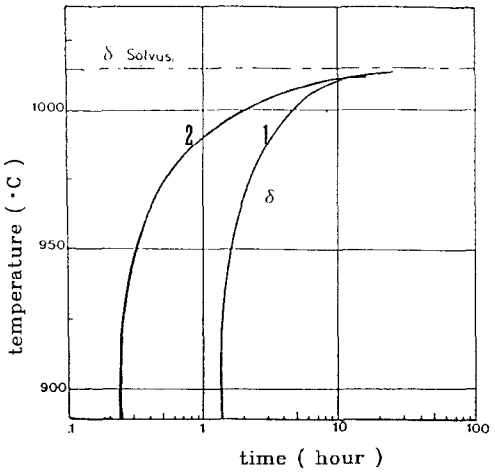

Fig.2: TTT–diagram : precipitation nose
1 ref. 1
2 Snecma's results

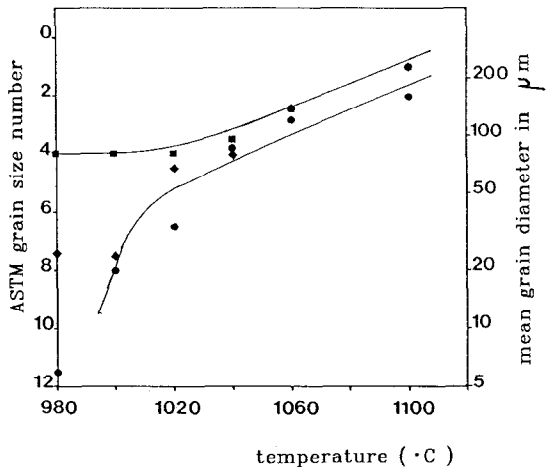

Fig.3: Grain–size vs annealing temperature after 1 hour for different initial microstructure.

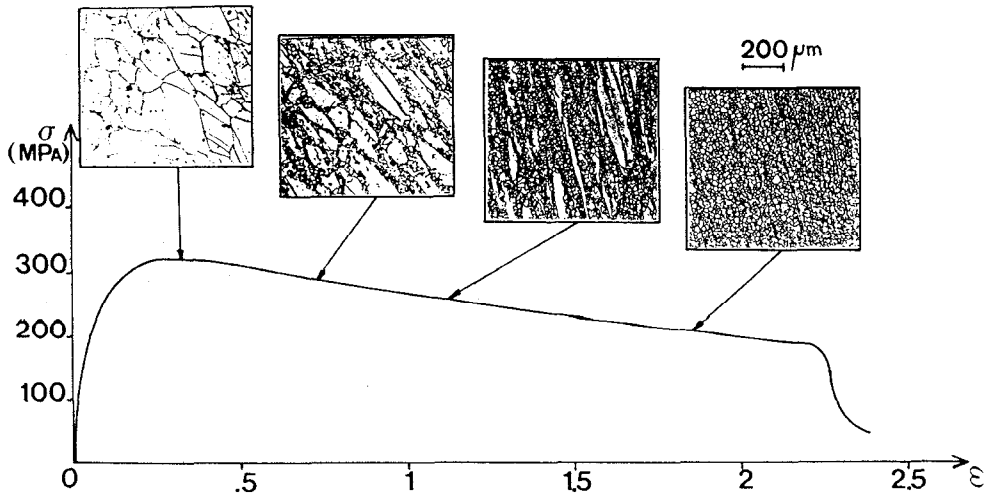

Fig.4: Microstructure and flow stress–evolution during dynamic recrystallization.
Conditions of deformation: torsion/1050°C/3.3s^{-1}

properties depend principally on grain size, we shall focus our attention on grain size prediction, the difficulties being that grain evolution interacts with the evolution of other metallurgical features, such as δ phase and residual cold work.

Phase diagram

The phase diagram of Alloy 718 has been first established by Eiselstein [1] and shows the following features :
- above 1010°C at equilibrium, the only metallic phase is γ- austenite,
- the δ-solvus is determined to be at 1010°C. However, because of variations in Nb-content due to dentritic segregation, it can vary locally between 990°C and 1020°C. This δ-solvus range is reduced in good quality billets,
- δ precipitation does not occur very rapidly, except in a structure with a high residual cold-work level,
- γ"-solvus lies between 900°C and 925°C.

In comparison with these data, SNECMA's own determination of TTT diagram shows a rather important shifting of the precipitation nose towards the shorter times (fig.2).

The forge engineer may draw the following conclusions :
- above 1020°C grain growth will occur and will be limited only by carbide precipitation,
- between 970°C and 1020°C, grain growth may be inhibited by δ precipitates, but around 1000°C the resulting microstructure is very sensitive to dendritic segregation,
- cooling down and, more markedly, heating up will induce some δ precipitation
- normally, forging operations are conducted between 980°C and 1120°C in the single-phase domain or with a very small amount of δ phase.

This last remark is an additional justification for SNECMA's choice to model first the grain size evolutions, neglecting somehow the influences of δ phase and residual cold work.

Static recrystallization

Static recrystallization occurs mainly during the preheating and heating sequence before forging and also before quenching. The δ-solvus temperature separates two domains in the kinetics of grain growth (fig 3).

Above the δ-solvus (1020°C to take segregation into account) a near-equilibrium grain size is reached after an one-hour-annealing. Grain growth between 1 hour and 4 hours anneal is very limited and would lead to the same ASTM quotation due to the scatter of the conventional measuring method. This equilibrium grain size is independent of the initial microstructural state and depends only of the annealing temperature following the experimental correlation :

$$d = 75 \times \exp [0.015 (T - 1020)] \quad \text{with d in } \mu m \text{ and T in } °C$$

or $$GS = 4 + 0.015 (T - 1020) \quad \text{with GS in ASTM}$$

This formula is valid between 1020°C and 1100°C, and provided that initial grain size is finer than 75 µm.Its imprecision is ∓ 1 ASTM.
For shorter annealing time, it appears that a similar formula can be applied. But in this case the grain size would depend on the initial microstructure.

Below 980°C, for annealing durations representative of preheating sequences, the grain size does not vary at all. In between, grain size evolution would depend strongly on the initial microstructure, δ precipitate content and residual cold work. In particular, a strong dendritic segregation can lead to alternate bands with grain size variations up to 4 ASTM.

Dynamic recrystallization

When Alloy 718 is deformed above 950°C and at rates higher than 10^{-4} s^{-1}, the first grain refinement mechanism is dynamic recrystallization. An exemple of microstructural evolution is given on fig.4. Dynamic recrystallization starts at a critical strain ε_{cr}, just below the maximum flow stress value. Small refined grains appear at the prior grain boundaries. The recrystallized fraction increases with deformation, forming necklace and duplex microstructures. A steady-state fully recrystallized structure is reached at ε_s with an homogeneous grain size d_s. Modelling the microstructure after forging involves predicting the grain size of both the cold worked and the recrystallized grains as well as the recrystallized volume fraction.

Recrystallization threshold ε_{cr}. The value of the critical strain classically increases with strain rate ε and decreases with temperature. However a good correlation exists between the peak stress and the recrystallization threshold (fig. 5). For strain rate values representative of those for isothermal forging (10^{-3} s^{-1} < $\dot{\varepsilon}$ < 10^{-2} s^{-1}), ε_{cr} may be estimated to be smaller than 0.15. For conventional press forging ($\dot{\varepsilon} \approx 10^{-1}$ s^{-1}), ε_{cr} is around 0.2. No experimental results are available for strain rate values applicable to hammer forging (10 s^{-1} < $\dot{\varepsilon}$ < 100 s^{-1}) ; however fig. 6 shows that for $\dot{\varepsilon}$ = 6 s^{-1}, ε_{cr} is higher than 0.4 ; it is likely that, usually, ε_{cr} is so large that dynamic recrystallization is negligeable and only metadynamic recrystallization is to be considered. In all the cases ε_{cr} decreases very slowly with temperature (fig. 6).

Steady state grain size d_s. It is often found that d_s is a function of the Zener-Hollomon parameter

$$d_s^{-1} = k \log Z \qquad Z = \dot{\varepsilon} \exp Q/RT \qquad (1)$$

where Q is the self diffusion energy [2]. So that d_s is expected to decrease with ε and increase with T. In Alloy 718, the results are conflicting since, for instance, Camus et al. [3] found that d_s increases with $\dot{\varepsilon}$ in the range 4 x 10^{-2} s^{-1} to 4 s^{-1}, whereas we found no real dependance of d_s between 10^{-1} s^{-1} and 6 s^{-1} (table 1).

strain-rate (s^{-1})	.09	3.3	6.0.
grain size (ASTM)	9.5	9.0	9.5

Table 1: Evolution of grain size with strain-rate at 1050°C

Two reasons may explain this discrepancy. In most rheological torsion testings, the quench is reported to happen 1 or 2 seconds after the end of the deformation ; this time is longer than the deformation time when the strain rate is high (e.g. $\dot{\varepsilon}$ > 1 s^{-1}) ; so that one can suppose, and Camus [3] mentions some metallographical evidence of it, that at these fastest strain rates metadynamic recrystallization must occur before quenching. The second reason is that over $\dot{\varepsilon}$ = 0.1 s^{-1}, the deformation is almost adiabatic and that after a deformation ε = 1 the temperature rise can be as

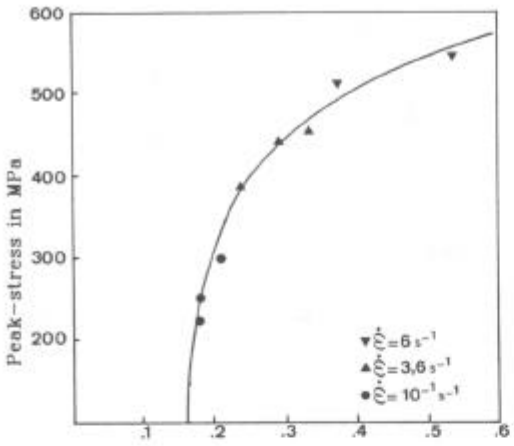

Fig.5: Peak-stress vs threshold-strain

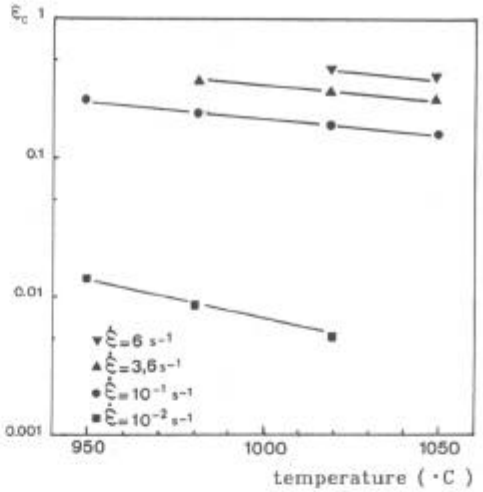

Fig.6: Threshold strain vs temperature and strain-rate.

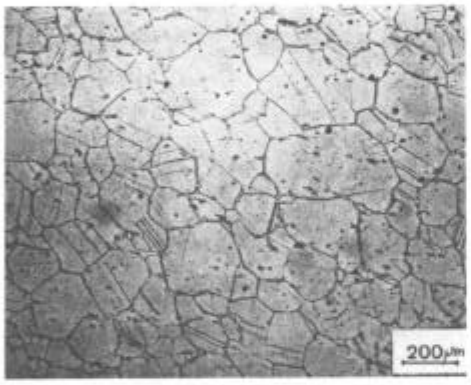

Water-quenched

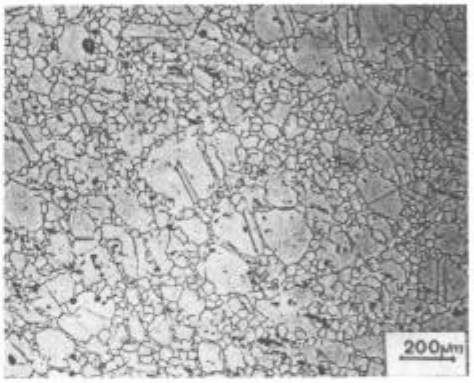

Air-cooled

Fig.7: Influence of the cooling-down rate on the recrystallized fraction.
Conditions of deformation: 1050·C/3.3$\bar{3}^{1}$s/0.14

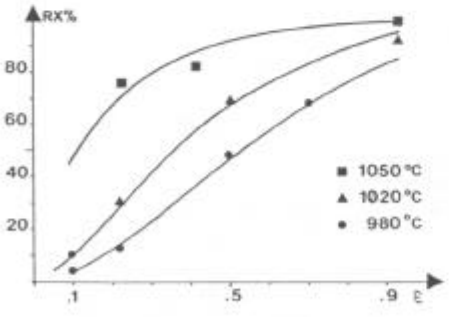

Fig.8: Metadynamic recrystallization. Evolution of recrystallized fraction with temperature and strain

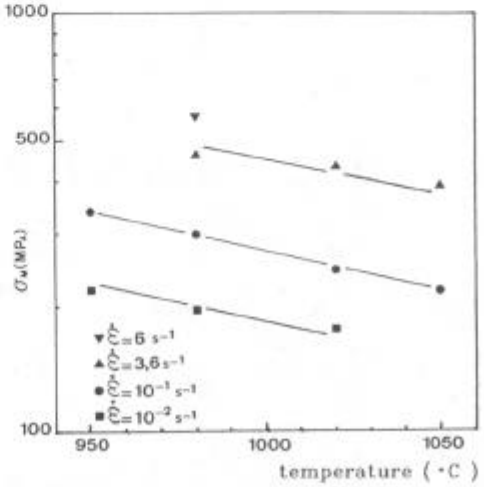

Fig.9: Peak-stress vs temperature and strain rate

high as 75°C. We can assume that relation (1) would be verified for quenching occuring very soon after the deformation ends and if one took into account the instantaneous temperature.

In the actual case where the cooling rate is slow, we found that the main parameter influencing d_s was the initial deformation temperature T. The experimental relationship between d_s and T when both dynamic and metadynamic recristallization are active, is given on table 2.

Steady state deformation ε_s. The determination of ε_s, suffers from the same difficulty than that of d_s : one has to compensate for adiabatic heating. Even in that case, the values reported in the litterature are so high, over 1,2 - 1,5, that they are reached very seldom during one forging operation. Dynamic recrystallization is to be continued by metadynamic recrystallization.

Metadynamic recrystallization

Metadynamic recrystallization is a static recrystallization process occuring just after the end of deformation ; but it is quicker since there is no intermediate cooling down and heating up leading to δ phase precipitation. Dynamic recrystallization results (see section above) show that in most cases, metadynamic recrystallization must occur to achieve a fully recrystallized state at the end of a forging. Fig 7 shows the difference in microstructural state after deformation, for two different cooling rate. In the slowly cooled specimens new grains have nucleated and grown at the expense of cold worked ones, leading to a necklace structure, whereas in the water-quenched specimens, these new recrystallized grains are to be seen only from place to place. For slowly cooled specimens, the recrystallized fraction depends on both initial deformation temperature and initial microstructure. Fig 8 shows this evolution for an initial microstructure of 3 ASTM. The recrystallized grain size is of the same order or a little finer than after dynamic recrystallization at the same temperature (table 2).

	grain size after ..... (ASTM)	
temperature (°C)	dynamic recrystallization	metadynamic recrystallization
1050	7	8.5
1020	8	10
980	9.5	11

Table 2: Evolution of grain size with recrystallization temperature.

Conditions of deformation:
dynamic recryst. : 3.3 s^{-1}/air quench
metadynamic recryst. : .1 s^{-1}/air cool

Metallurgical data base for Alloy 718

There are some difficulties in establishing an exhaustive metallurgical data base for forging purposes. Part of them arise from the measuring techniques of the microstructural parameters. For instance, no technique gives in reasonable time unquestionnable values for δ content and precipitate size for an exhaustive set of thermal and deformation conditions for the moment. Following this lack of reliable measurements, it becomes almost impossible to identify an existing precipitation or solutioning model. Other difficulties come from the rheological experiments. On one hand, one has to cope with very strong coupling between strain and temperature, so that at medium and high strain rates an isothermal experiment is unrealistic ; on the other hand, a correct freezing of the microstructure must be achieved in a shorter time than the deformation process itself. Generally this appears not to be the case.

As a consequence of these difficulties the metallurgical results are not reliable enough to feed physically established relationships between structural state variables and process variables but can give the general trends and some approached values describing the metallurgical structure resulting from the process.

Metallurgical modelling of disk hammer forging

The aim of this modelling is to provide a grain size prediction. The method consists in deriving the expected microstructure from the calculated strain distribution within the part, using an isothermal flow modelling. It has been initiated using rules which will be exposed further, then calibrated, comparing experimental results with the calculated microstructure.

As it does not take into account temperature and time effects, it is not a general model and is to be applied only for the process which it has been calibrated with. It is of no use for comparing two different processes as will be shown further. But it allows to compare different geometrical solutions for the forging of a part in a single tightly controlled process.

Metal flow model

At SNECMA's we use the finite element program FORGE2^R, developped in cooperation with the CEMEF (Ecole des Mines), which has already been extensively described elsewhere [4]. The main hypothesis for the calculations are : no gravity nor inertial forces, incompressibility and isotropy of the material, NORTON-HOFF viscoplastic behaviour ($\sigma_o = K\dot{\varepsilon}^m$), fluid boundary layer friction law ($\tau = \alpha \Delta V^p$), rigid dies.

Originally the program had an isothermal formulation. Now the thermal coupling has been incorporated. But the results presented here are only isothermal.

The flow rule for Alloy 718 is given on fig.9. We choose to represent only the peak stress as a function of strain rate only, including neither strain hardening nor softening. Strain hardening would result in a more uniform deformation within the part, so that calculations give rather conservative values. On the contrary, an eventual flow softening would increase strain localization, making the model inadequate. But, as we never experienced such a trend for Alloy 718 in the hot working range, the peak-stress approximation is considered to be coherent with the isothermal formulation.

The friction factors are chosen so as to be equivalent to a Tresca coefficient of m = .3 [5].

As we don't consider the time-dependance of temperature nor the one of metallurgical structure, we consider the hammer-ram velocity as constant.

Initial metallurgical data for grain size prevision

These rules derive from the results shown previously :

- grain size after preheating and heating is given in fig.3,

- depending on the deformation temperature and the strain level, the microstructural aspect will be unrecrystallized, duplex or fully recrystallized (fig.8),

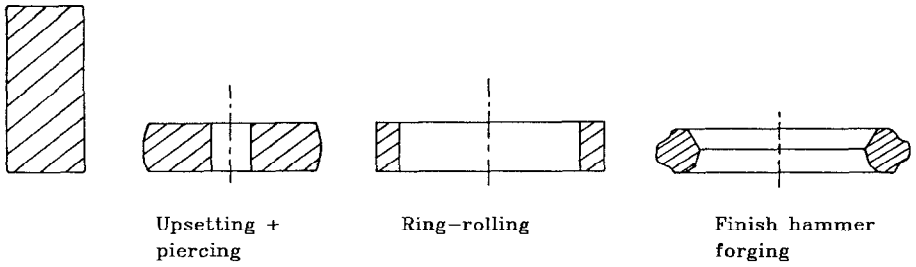

Fig.10: General forging sequence of a CFM56–LPT–disk

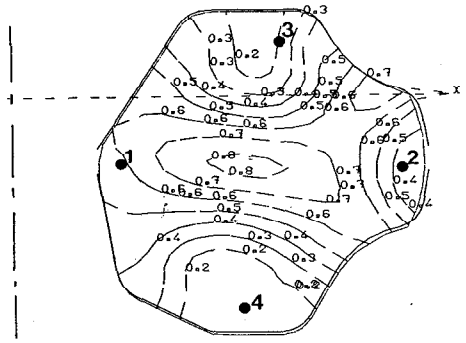

Fig.11: Final strain distribution in LPT–disk forging.

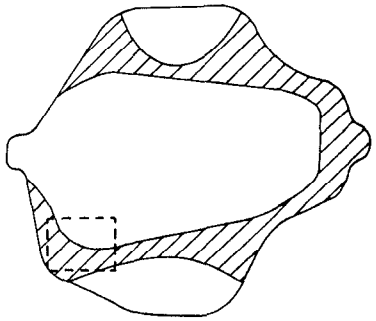

Dead zone(DZ)

100% Recrystallized zone (RX)

Duplex zone

forging temperature	Grain size ASTM RX	DZ
1100°C	6	2
1060°C	7.5	4
1020°C	10	6

Fig.12: Mean microstructure distribution in a LPT –disk forging

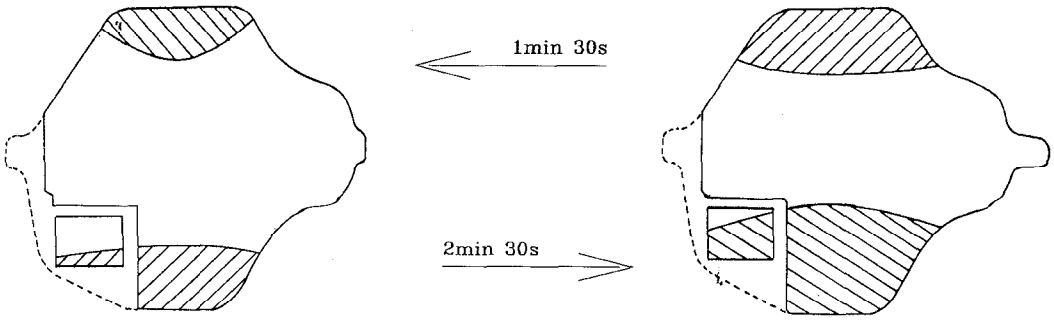

Fig.13: Dead–zone limits in relation with final forging duration.

- the main grain refinement mechanism is metadynamic recrystallization ; so that recrystallized volumic fraction will also depend on the cooling rate,

- the size of unrecrystallized grains in the dead zones remains unaffected during the forging,

- the size of recrystallized grains is given on table 1.

Turbine disk forging

Through the years, the CFM-56 engine has been improved in terms of efficiency and thrust leading to an increasing of the disks temperatures and stresses. During this period the forging temperature has been reduced to improve material capabilities. This section will show an example of forge modelling in order to control the microstructure in an Alloy 718 -low pressure turbine (LPT) disk.

The general forging sequence consists in an upset + piercing stage, a ring-rolling operation and a finishing hammer forging (fig 10). Up to now we conduct all the forging operations above δ-solvus, so that we consider that the final microstructure results mainly from the last operation. We have thus modelled only the finishing hammer forging. Mechanical specifications are particularly severe at the rim, the bore and at both flanges.

Numerical modelling

The engineering strain at the end of the forging operation is represented in fig.11. In most of the volume, especially at the bore and at the rim, the strain level is higher than 0.3, resulting through dynamic and metadynamic recrystallization in an almost fully recrystallized structure. However, two dead zones appear in the flanges, characterized by strain levels below 0.3.

Disk forging

Micrographs of forged disk sections show a good correlation between the calculated strain distribution and the type of microstructure: cold-worked, duplex or recrystallized at any tested temperature, but the recrystallized grain size in the real forging is finer than predicted by the rheological testing (fig. 12). This fact leads to the expected need for a calibration. It can be attributed to limited knowledge of the local temperature. Another local temperature effect is frequently observed at the surface of the forging, where a duplex structure appears, despite a high strain level (fig.10 and 11 : location A).

The prediction of the dead zone locations can be altered by a change in the process as shown on fig.13. The time between two blows has been increased in the second process so that the forging operation lasts 2 min 30 s instead of 1 min 30 s, resulting in a final skin temperature below 900°C. The temperature at the end of the forging has thus become insufficient to recrystallize metadynamically and the dead zones have increased.

Conclusion

Metallurgical experimentations have been performed to study elementary mechanisms of grain growth and refinement. Above δ-solvus, despite conflicting results, one can derive qualitative rules to predict grain size evolution in static, dynamic and metadynamic evolution.

Using an isothermal metal flow modelling and the metallurgical rules one can obtain a useful grain size prediction. In particular, dead zone locations may be deduced. However in order to give the recrystallized grain size, the model has to be calibrated with real forgings.

SNECMA has integrated this modelling in its forging practice in order to analyze its present production and the design of new forgings.

[1] H.L. EISELSTEIN " Metallurgy of a Columbium - Hardened Nickel-Chromium-Iron Alloy " Advances in the Technology of Stainless Steels and Related Alloys, ASTM-STP 369 (1965), 62-79

[2] M. UEKI, S. HORIE, T. NAKAMURA "Factors Affecting Dynamic Recrystallization of Metals and Alloys ", Materials Science and Technology, May 1987, vol. 3, 329-337.

[3] Gerald CAMUS, Bernard PIERAGGI, and François CHEVET "Hot Deformation and Recrystallization of Inconel 718 ", Symposium proceedings : formability and Metallurgical structures, October 86, Orlando, PMS 87, ed. A.K. GACHDEV, J.D. EMBURY, p. 305 - 326

[4] Yves GERMAIN, Pierre-Etienne MOSSER, "Finite element analysis of shaped lead-tin disk forgings"
NUMIFORM 86, A.A. BALKEMA, ROTTERDAM, BOSTON

[5] Pierre-Etienne MOSSER, Yves GERMAIN, "Le modèle de forgeage isotherme FORGE2", 65th SMP AGARD - CP 426, CESME 2-4 OCTOBER 1987